CHAPTER VII
SCALE INHIBITION STUDY BY TURBIDITY MEASUREMENT

7.1 Abstract

The concept of a critical supersaturation ratio (CSSR) has been used to characterize the effectiveness of different types of scale inhibitors, inhibitor concentration, and precipitating solution pH in order to prevent the formation of barium sulfate scale. The scale inhibitors used in this work were Aminotri methylene phosphonic acid (ATMP), Diethylenetriaminepenta methylene phosphonic acid (DTPMP), and Phosphinopolycarboxylic acid polymer (PPCA). The CSSR at which barium sulfate precipitates was obtained as a function of time for different precipitation conditions and was used as an index to evaluate the effect of the precipitation conditions. The results showed that the CSSRs decrease with increasing elapsed time after mixing the precipitating solutions, but increases with increasing scale inhibitor concentration and solution pH. The CSSR varies linearly with the log of the scale inhibitor concentration and with the precipitating solution pH. A SEM analysis showed that the higher the scale inhibitor concentration and solution pH, the smaller and more spherical the $BaSO_4$ precipitates. Analysis of the particle size distribution revealed that increasing the elapsed time, the scale inhibitor concentration, and precipitating solution pH produce a broader particle size distribution and a smaller mean diameter of the $BaSO_4$ precipitates. DTPMP and PPCA were the most effective $BaSO_4$ scale inhibitors per ionizable proton and the most effective on a concentration basis, respectively.

7.2 Introduction

Scale deposition in petroleum reservoirs is a common problem in the production of oil and gas. Waterflooding of the reservoirs is the most widely used process for improving oil productivity. In an offshore system, seawater is injected into the reservoir to displace the remaining oil in the reservoir. Water that exists

naturally within the pores of rock, called formation water, usually contains significant amounts of divalent cations such as calcium (Ca^{2+}), magnesium (Mg^{2+}), barium (Ba^{2+}), and strontium (Sr^{2+}). These cations can react with anions, such as sulfate (SO_4^{2-}) and carbonate (CO_3^{2-}), in the injected brine water to produce insoluble scales. Continuous scale growth can eventually lead to the blockage of the pores in the oil flow pathways which damages the production system, and decrease productivity. This problem can cost the oil producers millions of dollars per year in productivity loss and overhaul expense.(Allen and Robert, 1989; He *et al.*, 1996; Dunn *et al.*, 1999)

The most practical and economical method to combat this scaling problem is the use of chemical scale inhibitors. The scale inhibitors have the ability to prevent or to slow the nucleation and growth of the scale. In many cases, the amount of scale inhibitors required is very low, ca. less that 50 ppm. Above a certain threshold concentration, scale inhibitors can reduce the tendency for crystallization or completely prevent scale formation and growth by disrupting the thermodynamic stability of growing nuclei, causing dissolution of nucleated scale and/or interfering with the crystal growth process, resulting in blockage of the growing sites.(Graham *et al.*, 2003)

Commercial scale inhibitors are often claimed to be efficient at low dosages for a wide range of solution pH values and temperatures. Scale inhibitor screening tests in the laboratory are used for selecting the appropriate scale inhibitor and conditions before using it in the field.

This research demonstrated the application of the concept of the critical supersaturation ratio (CSSR) to study scale inhibition and evaluate scale inhibitor type, concentration and pH effectiveness using the formation of $BaSO_4$ as example. The CSSR is a supersaturation ratio, above which the turbidity increases steeply with time due to nucleation and growth of scaling particles. Furthermore, the morphology, the elemental analysis, and the particle size distribution of the resulting $BaSO_4$ precipitates were also comparatively examined. An understanding of scale inhibition kinetics to predict scale formation, as well as to prevent the formation of scale were presented.

7.2.1 Calculation of Supersaturation Ratio

The degree of mineral supersaturation can be quantified by a supersaturation ratio (SR), which is the ratio of the ionic activity product (i.e., barium and sulfate) to the solubility product (i.e., the K_{sp}). In case of ideal solutions, the SR must be higher than one for precipitation to occur. When the SR is equal to one, the solution is saturated. Mineral dissolution occurs when the solution is undersaturated (SR<1). The SR for $BaSO_4$ can be expressed as:

$$SR = \frac{a_{Ba^{2+}} \cdot a_{SO_4^{2-}}}{K_{sp}} \tag{7.1}$$

where a denotes activities and K_{sp} is the solubility product. For barium sulfate the solubility product is

K_{sp} of $BaSO_4$ = 1.08 x 10^{-10} M^2 at 25°C

The activity of species "i" is defined as:

$$a_i = f_i \cdot C_i \tag{7.2}$$

where a_i = activity of i-valent ions (M), (i.e. Ba or SO_4)

C_i = concentration of i-valent ions (M)

f_i = activity coefficient of i-valent ions

Substituting Eq. (7.2) into (7.1), results:

$$SR = \frac{f_{Ba^{2+}} \cdot f_{SO_4^{2-}} C_{Ba^{2+}} C_{SO_4^{2-}}}{K_{sp}} \tag{7.3}$$

In order to determine the activity coefficient in dilute solutions, the Debye-Huckel equation is used (Perrin and Dempsey, 1974).

$$\log f_i = -\frac{AZ^2 I^{0.5}}{1 + I^{0.5}} + 0.1 \cdot Z^2 I \tag{7.4}$$

where Z = charge of ion

I = ionic strength (M)

A = a temperature dependence constant (at 25°C: A = 0.512)

The ionic strength is given by the summation as:

$$I = \frac{1}{2} \sum C_i Z_i^2 \tag{7.5}$$

rewriting Eq. (7.3) as:

$$SR = \frac{C_{Ba^{2+}} C_{SO_4^{2-}}}{K_{sp}^*} \tag{7.6}$$

where

$$K_{sp}^* = \frac{K_{sp}}{f_{Ba^{2+}} f_{SO_4^{2-}}} \tag{7.7}$$

This form allows one to calculate K_{sp}^* as a function of the ionic strength of the solution (see Table 7.1).

Table 7.1 K_{sp}^* values as a function of ionic strength of the solution.

Ionic Strength (M)	0.004	0.006	0.008	0.010
K_{sp}^* ($M^2 \times 10^{-10}$)	1.88	2.10	2.31	2.50

Equation 7.6 and Table 7.1 show that not only the concentration of barium and sulfate ions, but also the ionic strength can affect the supersaturation ratio.

7.2.2 Critical Supersaturation Ratio

The typical behavior of the turbidity as a function of the supersaturation ratios is shown in Figure 7.2. The turbidity remains constant up to the point where the CSSR has been reached. Although the supersaturation ratio values below the CSSR are much greater than 1, no precipitation of $BaSO_4$ was observed after an elapsed time of 2 h after mixing the precipitating solutions. For supersaturation ratios greater than the CSSR, the concentration of the $BaSO_4$ precipitate is well represented by a linear relation to the CSSR as shown in Figure 7.1.

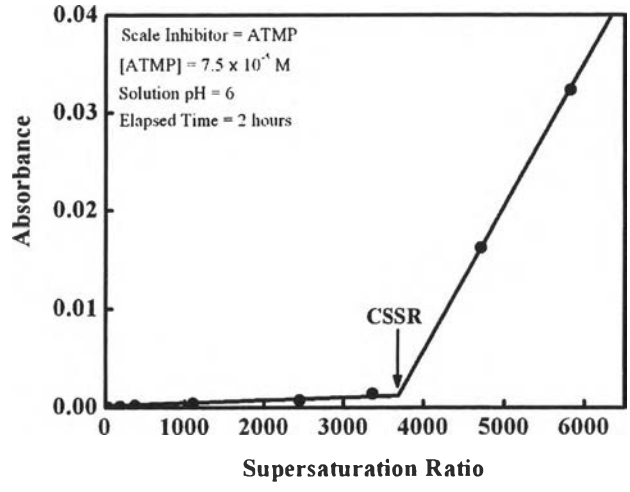

Figure 7.1 Solution turbidity (as absorbance of light at 250 nm) as a function of the supersaturation ratio.

7.3 Materials and Methods

7.3.1 Materials

Three commercial grade scale inhibitors were used in this study: ATMP, DTPMP, and PPCA. The chemical structures of selected inhibitors are shown in Figure 7.2. ATMP (Dequest® 2000) and DTPMP (Dequest® 2060) obtained from Solutia are the phosphonate scale inhibitors having three and five active phosphate groups, corresponding to six and ten ionizable protons, respectively. PPCA (Bellasol® S30) obtained from Biolab is a polymeric scale inhibitor and contains twenty-five ionizable protons. Analytical grade barium chloride dihydrate ($BaCl_2.2H_2O$) and sodium sulfate (Na_2SO_4) were obtained from Fisher Scientific, Inc. Solutions of these salts in ultrapure deionized water were used as precipitating constituents to form $BaSO_4$ precipitates.

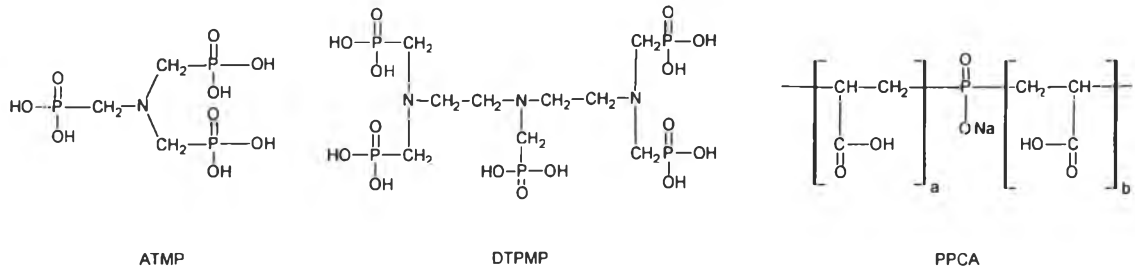

Figure 7.2 Chemical structure of ATMP, DTPMP and PPCA.

7.3.2 Determination of CSSR

Batch experiments to study $BaSO_4$ inhibition were carried out in 20 ml vials at room temperature (25°C). Stock solutions of $BaCl_2$ and Na_2SO_4 were adjusted to the desired pH values. Na_2SO_4 solution was first mixed with the scale inhibitor solution. Next, the $BaCl_2$ solution was added to attain various supersaturation ratios. All vials were vigorously shaken for complete mixing. The solution turbidity (as absorbance of light at 250 nm) was determined at pre-established intervals.

The critical supersaturation ratio (CSSR) is a supersaturation ratio, above which the turbidity increases steeply due to nucleation and growth of $BaSO_4$ particles. Scale inhibitors can affect either the nucleation rate and/or the growth rate of precipitation. The turbidity measurement alone cannot differentiate between these two phenomena and therefore we make no assumptions about which of these possibilities regulates the formation of precipitates. Effective scale inhibition occurs when the CSSR obtained in the presence of inhibitor exceeds the CSSR when no inhibitor is present.

7.3.3 Morphology Analysis of $BaSO_4$ Precipitates

Solutions described in section 7.3.2 were placed on 0.22 μm membrane filters to separate suspended $BaSO_4$ particles from the solution. The $BaSO_4$ precipitates on membrane filters were then washed with ultrapure deionized water, dried and placed onto sample holders for the morphological analysis. The $BaSO_4$

precipitates formed at different precipitating conditions were examined by using a Scanning Electron Microscope (Philips, XL30 FEG SEM).

7.3.4 Particle Size Distribution Analysis of $BaSO_4$ Precipitates

A Centrifugal Particle Size Distribution Analyzer, CAPA-500, manufactured by Horiba Instruments Inc. was utilized to determine the particle size distribution of the $BaSO_4$ precipitates.

7.4 Results and Discussion

In this study, the CSSR of the barium sulfate was systematically determined in the presence of three scale inhibitors including ATMP, DTPMP, and PPCA. After mixing the precipitating solution, the effects of the elapsed time to the observe point of precipitation were studied as a function of the solution pH, concentration, and the scale inhibitor type. The CSSR in the absence of scale inhibitors are used as a baseline for comparison. The morphological structure, elemental analysis and particle size distribution of the resulting $BaSO_4$ precipitates were also comparatively studied.

7.4.1 Effect of Elapsed Time on CSSR

The effect of elapsed time on the formation of $BaSO_4$ precipitates is shown in Figure 7.3. The elapsed times in this study varied between 2 h and 3,268 h. As the elapsed time increased, a quick reduction of CSSR was observed for elapsed times up to 200 h, but for elapsed times greater than 500 h, the CSSR remained virtually constant as shown in Figure 7.4.

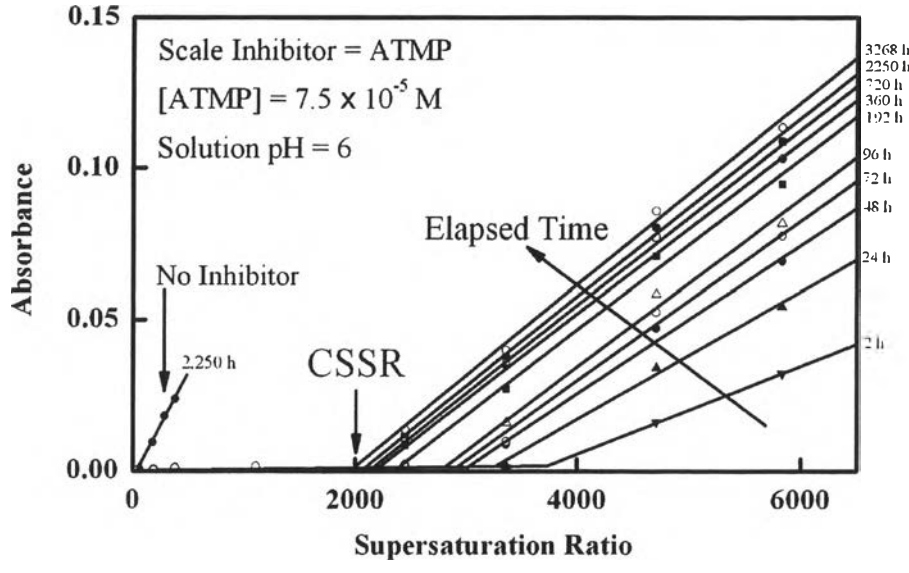

Figure 7.3 Concentration of $BaSO_4$ precipitates as a function of the supersaturation ratio and elapsed time.

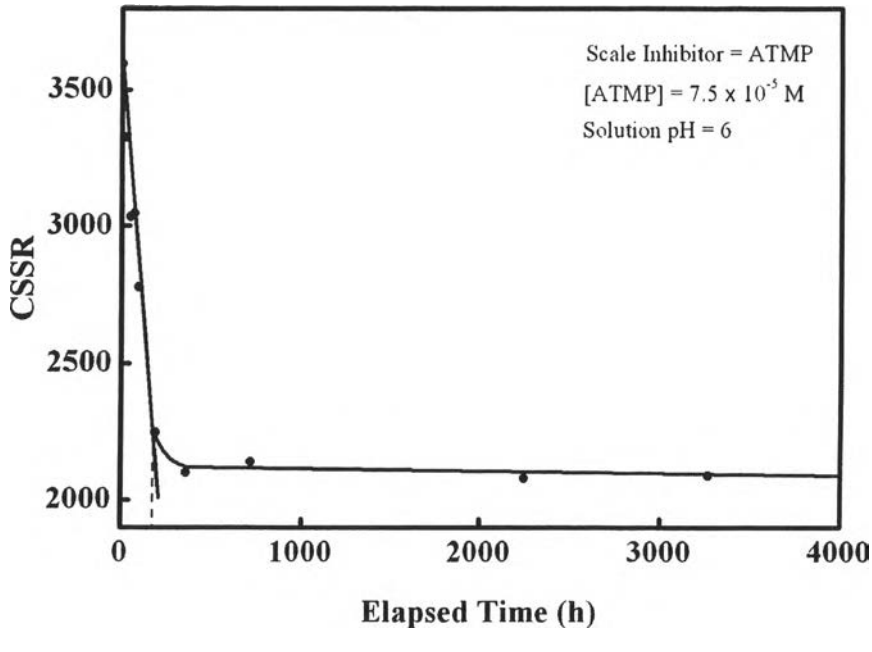

Figure 7.4 Variation of the CSSRs with the elapsed times after mixing the precipitating solutions.

7.4.2 Effect of Solution pH on CSSR

The effect of solution pH on the CSSR was examined both in the absence of inhibitor and at an inhibitor concentration of 7.5×10^{-3} M. The values of the solution pH studied were 4, 6, and 8 which correspond to the pH range used in the oilfield.(Yuan *et al.*, 1993) Figure 7.5 shows the variation of the CSSR with elapsed times at different pH values. No affect of pH on barium sulfate precipitation was found in the absence of inhibitor while it can be clearly seen that in the presence of inhibitor, the CSSR at pH 4 is significantly less than that of pH values of 6 or 8. For a phosphonate inhibitor such as ATMP, the absorption of at least two active phosphonate groups on the surface of the scale is required for the inhibition of barium sulfate.(Benton *et al.*, 1993) The degree of deprotonation of ATMP increases with increasing solution pH as shown in Figure 7.6. The deprotonation of the scale inhibitors appears to play a significant role in inhibition. At low pH values, ATMP exhibits a low degree of deprotonation, which reduces adsorption capacity on $BaSO_4$ precipitates. Consequently, at low pH conditions the inhibitor is less effective in slowing $BaSO_4$ particle growth and as a result lower CSSR values were observed.

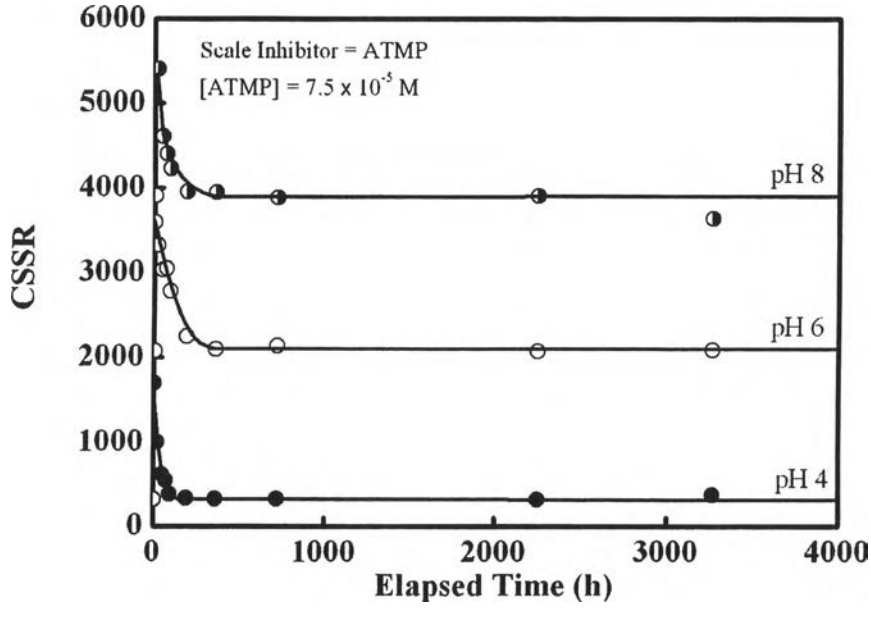

Figure 7.5 Variation of the CSSRs with elapsed time at different solution pHs.

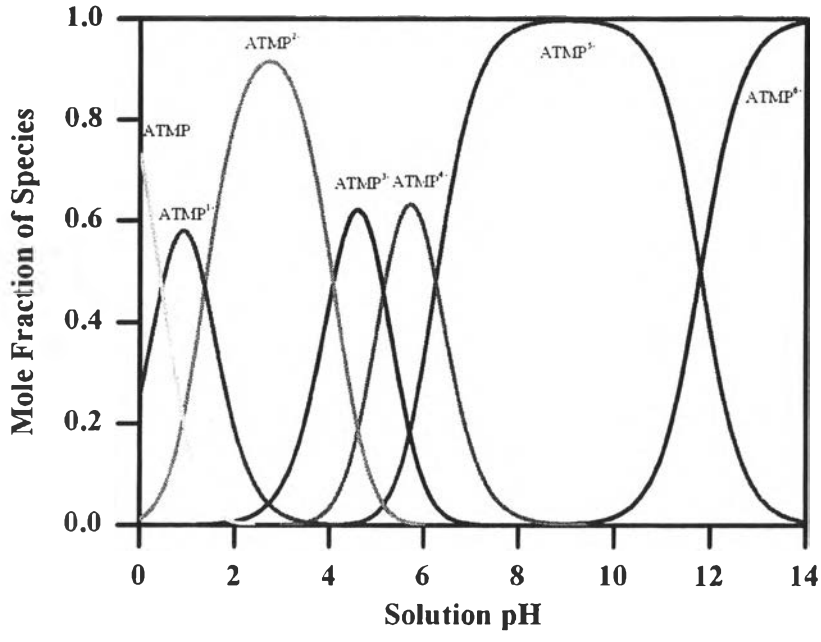

Figure 7.6 Deprotonation curves of ATMP and the resulting species composition.

The CSSRs are found to vary linearly with solution pH as shown in Figure 7.7 for the elapsed times of 24 h and of 2,250 h. This correlation can be used as a guideline in actual oil production operations, because selecting the appropriate pH can target a CSSR corresponding to a desired squeeze time. At any given elapsed time, the region under and above each curve in Figure 7.7 represents the no-precipitation and precipitation zones, respectively.

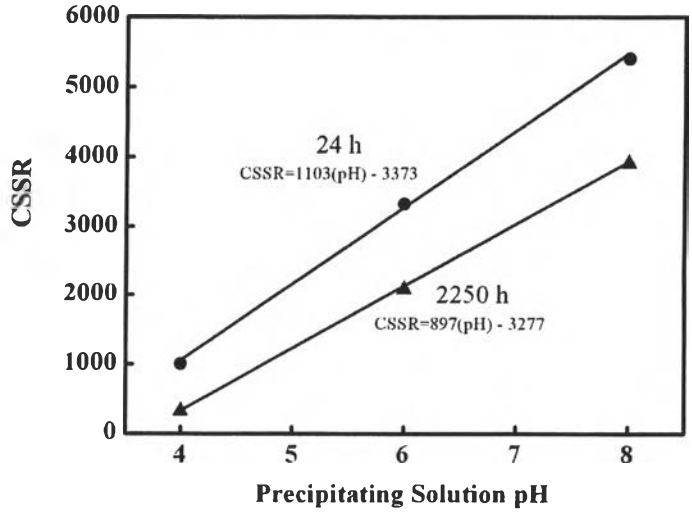

Figure 7.7 Effect of solution pH on CSSR.

7.4.3 Effect of Scale Inhibitor Concentration on CSSR

The effect of the scale inhibitor concentration on the CSSR was determined at a solution pH of 6 in both the presence and the absence of ATMP, DTPMP, and PPCA. The concentrations of these scale inhibitors were in range of 2.5×10^{-5} to 7.5×10^{-3} M which are in the concentration range used in oilfield operations. The effectively lowest concentration limit of scale inhibitor to exhibitthe scale inhibition is called, threshold concentration.(Sorbie *et al.*, 1994; Putnis *et al.*, 1995). However, a very high scale inhibitor concentration such as 7.5×10^{-3} M may occasionally be used in some oilfields with extremely serious scaling problems. Figure 7.8 shows the variation of the CSSRs with elapsed times for various concentrations of ATMP and for one without ATMP. Similar results were observed in the presence of both DTPMP and PPCA scale inhibitors.

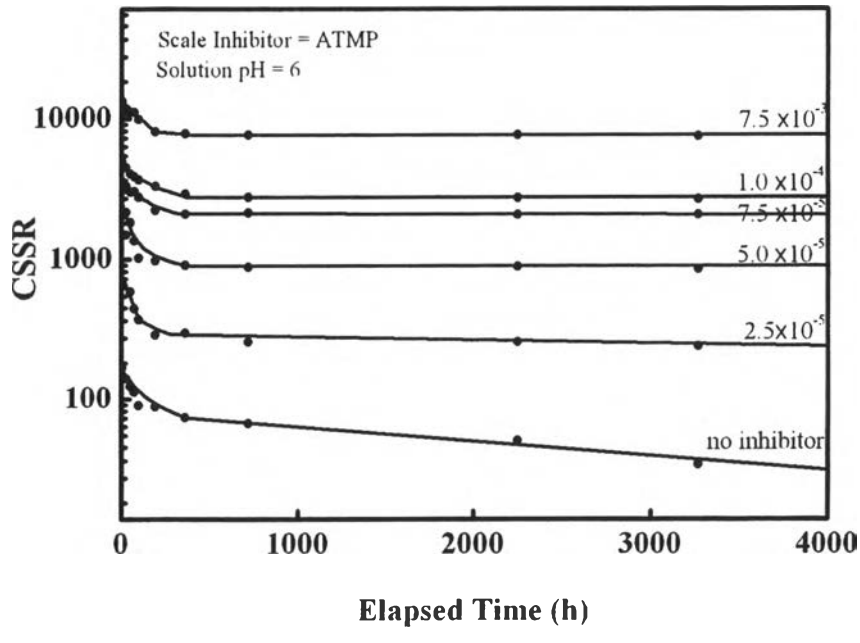

Figure 7.8 Variation of CSSRs with elapsed times at different scale inhibitor concentrations.

The CSSRs observed in the presence of the scale inhibitors are higher than in their absence. The CSSRs decreased with increasing elapsed time, and they tend to be constant at very long elapsed times. At low scale inhibitor (ATMP) concentrations, the CSSR decreases with elapsed time to a greater extent than at

higher concentrations, because at low scale inhibitor concentrations, a smaller number of active scale inhibitor molecules is available for adsorbing and blocking the formation of $BaSO_4$. Therefore, the $BaSO_4$ precipitates can form and grow more easily. In the absence of scale inhibitors, the CSSR tends to decrease continuously and gradually, until it reaches the solubility product (K_{sp}) at an extremely long elapsed time after mixing. At elapsed times between 24 to 2,250 h, the CSSR was found to vary linearly with the log of scale inhibitor concentration as demonstrated in Figure 7.9.

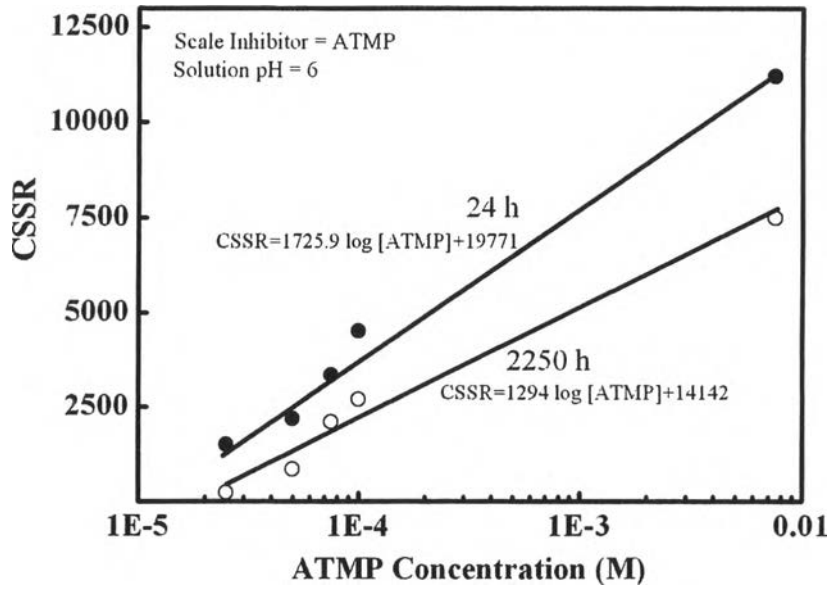

Figure 7.9 Effect of scale inhibitor concentration on CSSR.

7.4.4 Effect of Type of Scale Inhibitors on CSSR

The CSSR data for all 3 types of the scale inhibitors were normalized by the number of ionizable protons contained in each scale inhibitor species in order to exclude the effect of different amounts of active sites per molecule of the inhibitor. Figures 7.10 and 7.11 show the variation of the normalized CSSR with elapsed time for ATMP, PTPMP and PPCA, respectively. It can be seen that for short elapsed times the CSSR decreased rapidly with increasing elapsed time for all three inhibitors, but for long elapsed times the CSSR values decreased more slowly. At lower pH values, the CSSR remains virtually constant with increasing elapsed times.

At a solution pH in range between 4 to 8, DTPMP provided the greatest $BaSO_4$ inhibition efficiency compared to PPCA and ATMP. DTPMP increased the normalized CSSR from 684 at a low pH to 1,025 at a higher pH. Similarly, ATMP increased the CSSR from 53 to 651, and from 464 to 914 for PPCA. Because the formation of $BaSO_4$ in the presence of scale inhibitors are controlled by the adsorption of inhibitor molecules on the $BaSO_4$ crystal, the steric effects may play an important role on depressing the adsorption strength of large inhibitor molecules such as PPCA, resulting in a lower inhibition efficiency compared to DTPMP. ATMP is highly sensitive to solution pH as evidenced by the variation in the CSSR from 53 at pH 4 to 651 at pH 8. DTPMP provided the highest efficiency in the range 2.5×10^{-5} to 7.5×10^{-3} M of scale inhibitor concentrations at a constant solution pH of 6 as shown in Figure 7.11. The CSSR increased with increasing inhibitor concentration in the presence of PPCA and DTPMP. At a constant inhibitor concentration, the CSSRs decreased significantly in the first period of the elapsed time until it reached approximately 200 h and then became almost constant after 400 h. PPCA was more efficient in terms of the required concentration compared to others inhibitors as shown in Figure 7.12 perhaps because of the greatest number of ionizable protons (twenty five for PPCA, ten for DTPMP and six for ATMP) and thus its ability to block the greater number of the growth sites of $BaSO_4$ crystals.

7.4.5 Morphology and Particle Size Analysis

i. Effect of Elapsed Time

The particle size distribution of the $BaSO_4$ precipitates formed under the presence of ATMP at different elapsed times is shown in Figure 7.13. The results illustrate that a broader particle size distribution is observed with longer elapsed times. For a given precipitating condition, $BaSO_4$ particles of a smaller size form initially and then grow larger as the elapsed time increases. The mean diameter of the $BaSO_4$ particles increases with increasing elapsed time, up to 48 h. But, the mean diameter eventually reaches a plateau for elapsed times greater than 48 h, as shown in Figure 7.14.

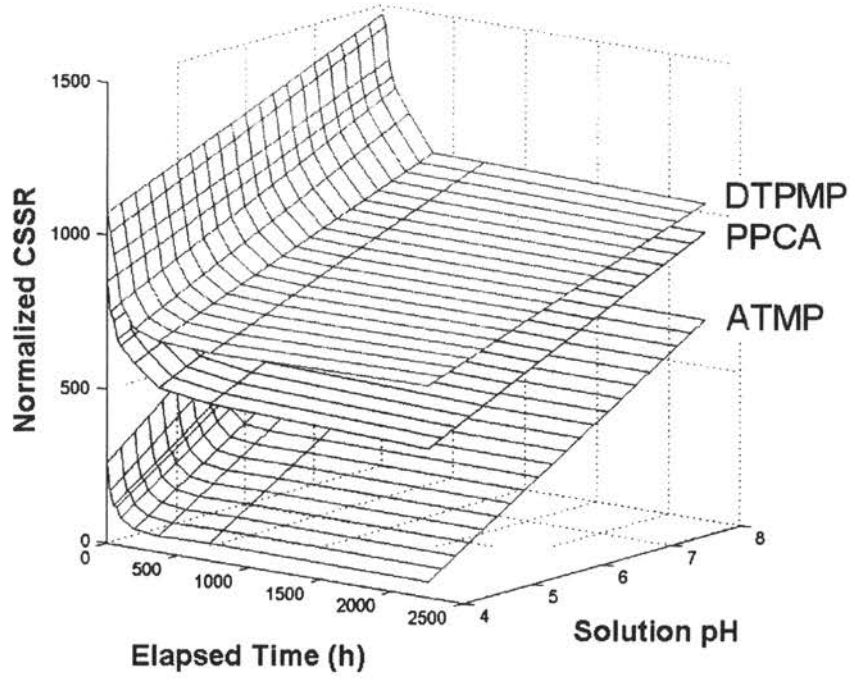

Figure 7.10 Effect of solution pH on the normalized CSSR for different types of scale inhibitor.

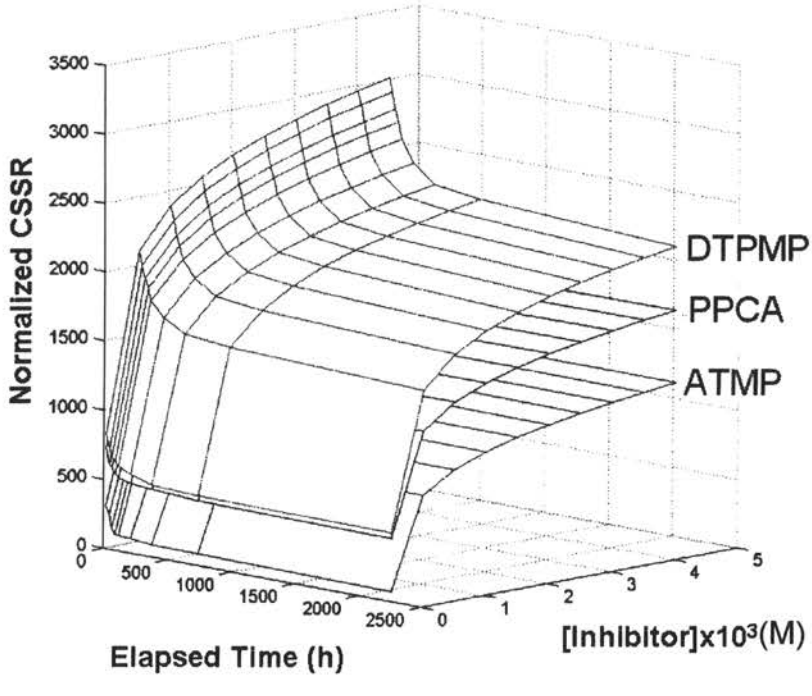

Figure 7.11 Effect of scale inhibitor concentration on the normalized CSSR for different types of scale inhibitor, pH 6.

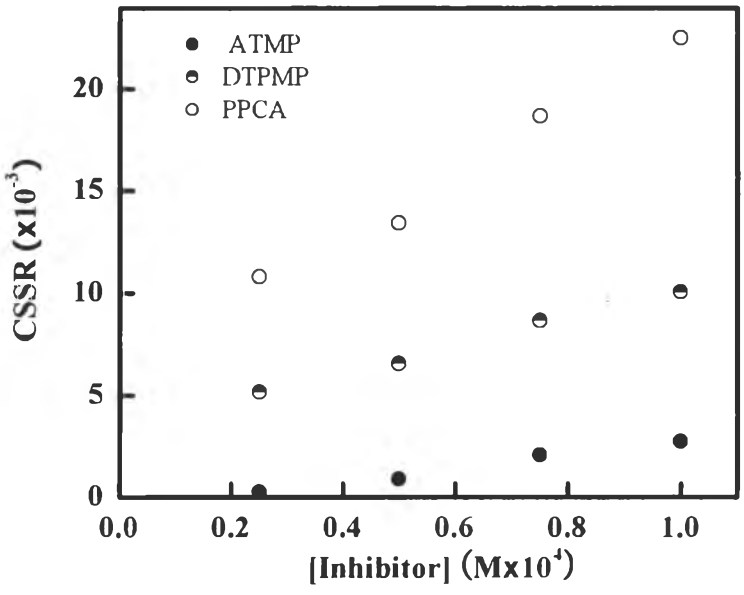

Figure 7.12 Effect of scale inhibitor concentration on the CSSR at equilibrium time for different types of scale inhibitor, pH 6

ii. Effect of Solution pH

The effect of precipitating solution pH on the particle size distribution and the mean diameter of the $BaSO_4$ precipitates is shown in Figures 7.15 and 7.16, respectively. The particle size distributions become broader and the mean diameters of the $BaSO_4$ particles become smaller with increasing solution pH.

Figure 7.17 shows examples of the morphology of the $BaSO_4$ precipitates formed at different solution pH values that were SEM micrographs. The higher the solution pH, the smaller and more spherical the $BaSO_4$ precipitate particles. Because the degree of deprotonation of a scale inhibitor is greater at higher solution pH values, there are more active sites to adsorb on the growing crystals causing blockage of crystal faces. This blockage results in smaller and more spherical $BaSO_4$ particles.

iii. Effect of Scale Inhibitor Concentration

Figures 7.18 and 7.19 display the effect of scale inhibitor concentration on the particle size distribution and the mean particle diameter of $BaSO_4$ precipitates, respectively. One observes a broader particle size distribution

and a smaller mean diameter of the $BaSO_4$ particles at higher scale inhibitor concentrations. At higher scale inhibitor concentrations, a greater adsorption of scale inhibitor molecules causes the blockage of the $BaSO_4$ particle growth, resulting in a smaller mean diameter of $BaSO_4$ particles.

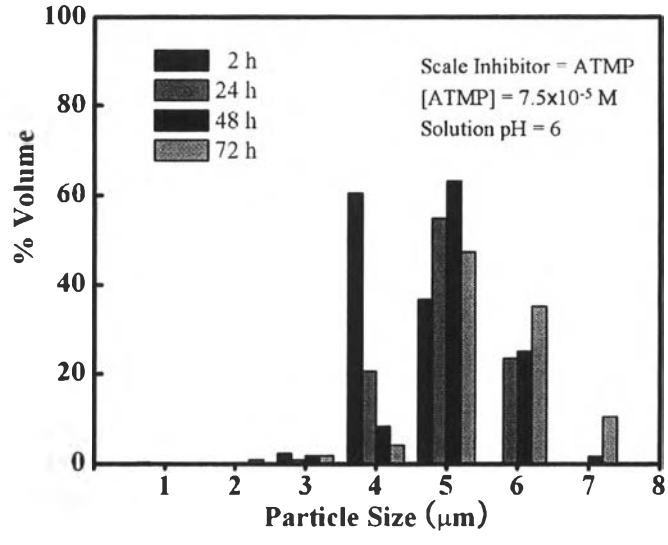

Figure 7.13 Effect of elapsed time on the particle size distribution of the $BaSO_4$ precipitates in the presence of ATMP.

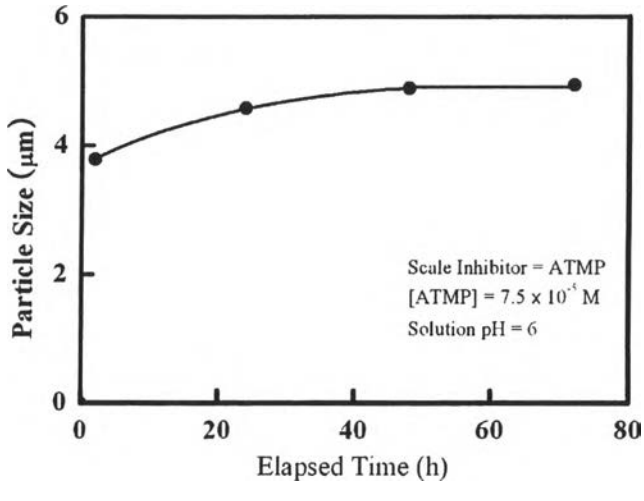

Figure 7.14 Effect of elapsed time on the mean diameter of the $BaSO_4$ precipitates in the presence of ATMP.

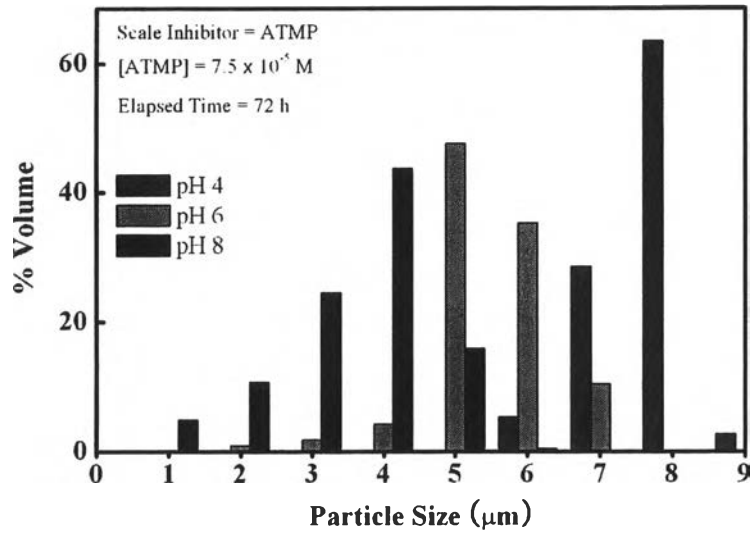

Figure 7.15 Particle size distribution of the $BaSO_4$ precipitates at various solution pH values.

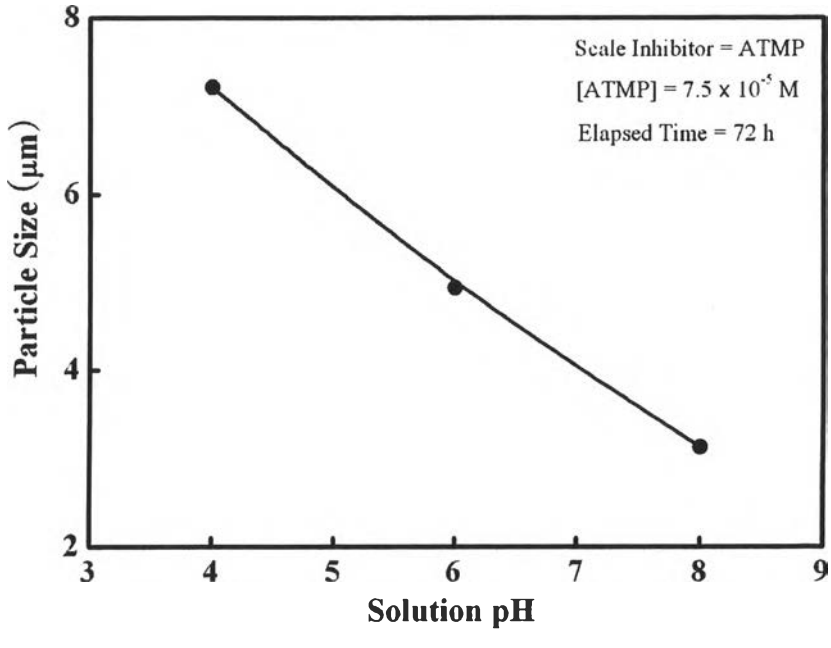

Figure 7.16 Effect of solution pH on the mean diameter of the $BaSO_4$ precipitates.

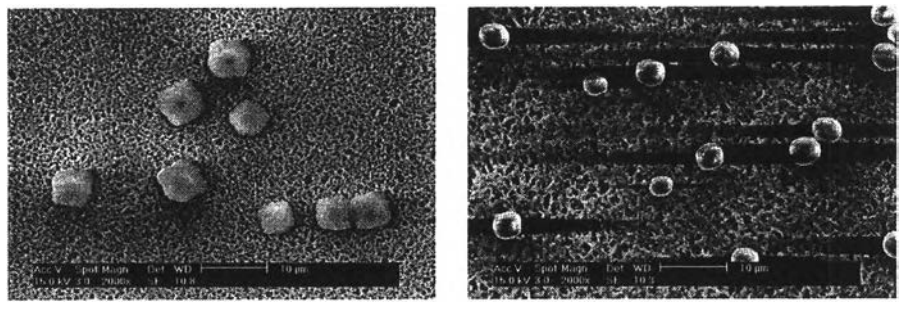

(a) pH 4, SR=5,832 (b) pH 6, SR=5,832

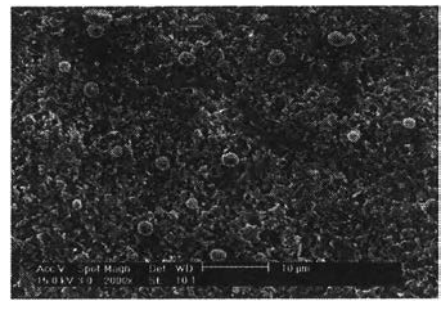

(c) pH 8, SR=7,402

Figure 7.17 Morphological structures of $BaSO_4$ precipitates at different solution pH values and at an elapsed time of 2 h in the presence of ATMP.

SEM micrographs of the morphologies of $BaSO_4$ precipitates formed under different ATMP scale inhibitor concentrations are shown in Figure 7.20. It can be seen that the concentration of scale inhibitors plays an important role on the morphological structure and the particle size of the $BaSO_4$ precipitates. The higher the concentrations of the scale inhibitor used, the smaller and more spherical were the $BaSO_4$ precipitates.

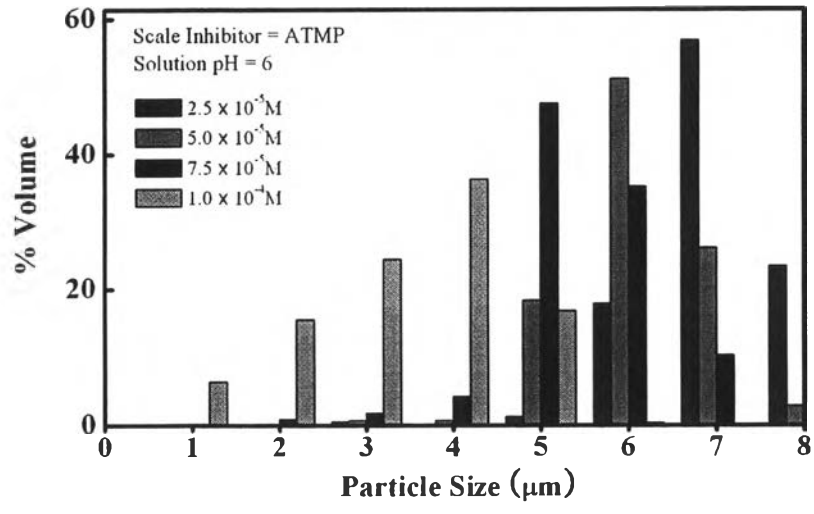

Figure 7.18 Effect of scale inhibitor (ATMP) concentration on the particle size distribution of $BaSO_4$ precipitates.

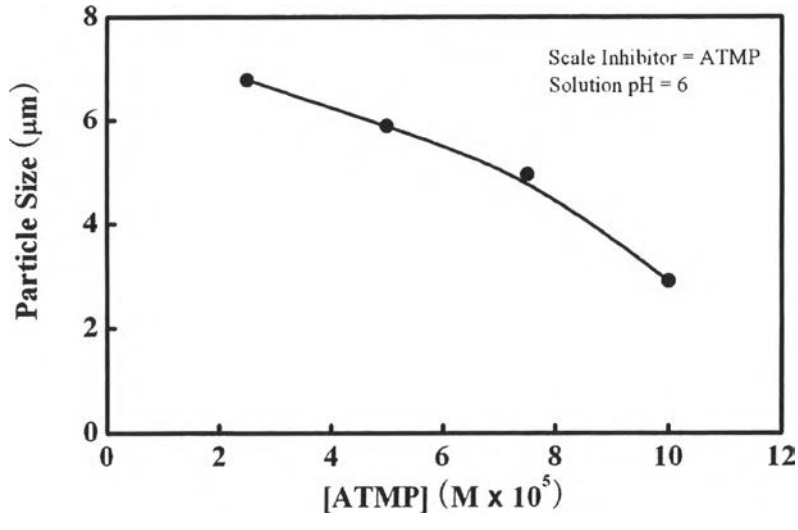

Figure 7.19 Effect of scale inhibitor (ATMP) concentration on the mean diameter of $BaSO_4$ precipitates.

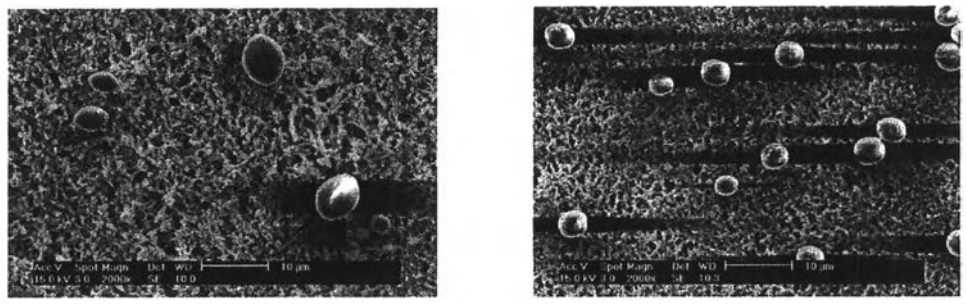

(a) [ATMP] = 2.5 x 10^{-5} M, SR=6,515 (b) [ATMP] = 7.5 x 10^{-5} M, SR=5,832

Figure 7.20 Morphological structures of $BaSO_4$ precipitates formed at different scale inhibitor concentrations of ATMP at an elapsed time of 2 h.

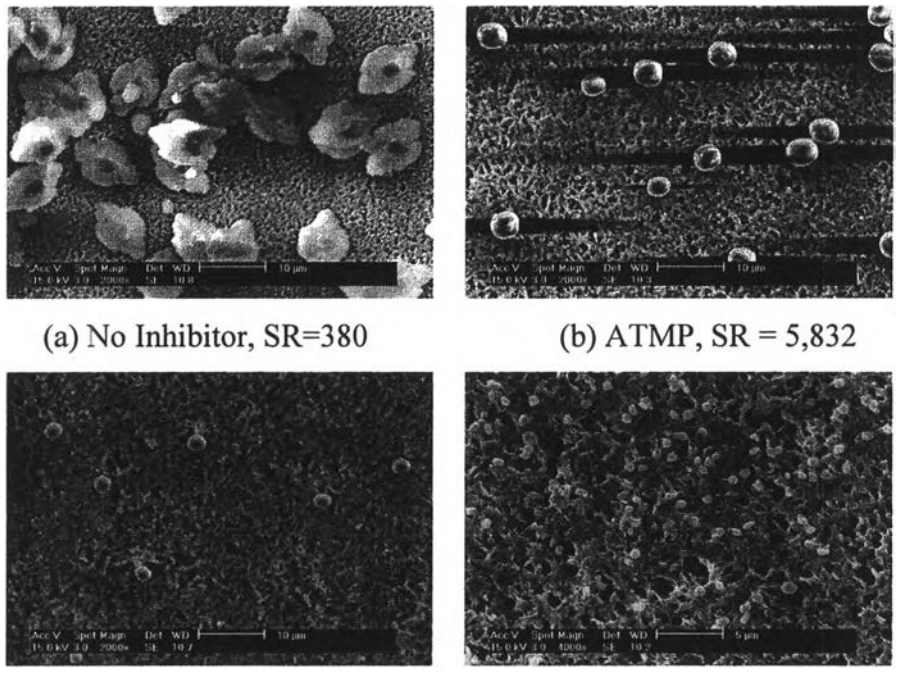

(a) No Inhibitor, SR=380 (b) ATMP, SR = 5,832

(c) DTPMP, SR = 17,500 (d) PPCA, SR = 40,844

Figure 7.21 Morphological structures of $BaSO_4$ precipitates in the presence of different scale inhibitors at an elapsed time of 2 h.

iv. Effect of the Type of the Scale Inhibitor

As described earlier, the presence of scale inhibitors has a significant effect on the morphological structure of $BaSO_4$ particles formed in solution. When no inhibitor is present the shape of the $BaSO_4$ crystal is plate-like, as seen in Figure

7.21a. However when any of three inhibitors are added to $BaSO_4$ solution, the crystal shape is no longer plate-like and instead appears more spherical as shown in Figure 7.2.

7.5 Conclusions

Batch $BaSO_4$ precipitation experiments were carried out in the absence and presence of different scale inhibitors, ATMP, DTPMP, and PPCA. The concept of the critical supersaturation ratio CSSR was defined to characterize the effectiveness of the scale inhibitor in terms of type, concentrations and solution pH to affect the scale inhibition of $BaSO_4$.

The types of scale inhibitor and precipitating conditions have a significant effects on the CSSR, the morphological structure, the particle size and size distribution of the $BaSO_4$ precipitates. In the presence of the scale inhibitors, the CSSR initially decreased sharply with increasing the elapsed time, and then, decreased at a diminishing rate until it reached a virtually constant value. However, in the absence of the scale inhibitors, CSSR continuously and gradually decreased until it reached the solubility product.

The higher the scale inhibitor concentration, the higher effectiveness of the $BaSO_4$ precipitation inhibition appaered, as manifested by an increase in the CSSR with increasing scale inhibitor concentration. The CSSR was found to be a linear function of the log of the scale inhibitor concentration. Additionally, the higher the solution pH, the higher effectiveness of the $BaSO_4$ precipitation inhibition was and the CSSR was found to increase linearity with the solution pH.

The addition of the scale inhibitors to a static precipitating solution resulted in smaller and more spherical $BaSO_4$ particles formed than that in the absence of the scale inhibitors. Higher scale inhibitor concentrations and solution pHs produced $BaSO_4$ precipitate particles with a smaller size, a more spherical shape and with a broader particle size distribution.

DTPMP, which contains ten ionizable protons per molecule, was the most effective $BaSO_4$ scale inhibition based on the CSSR per number of ionizable protons, compared to either PPCA or ATMP, which have twenty-five and six ionizable

protons, respectively. The PPCA inhibitor was the most effective inhibitor on the basis of concentration.

7.6 References

Allen, T. O. and Robert, A.P. (1989) Scale deposition, removal and prevention. Production Operations: Well Completions, Walkover and Stimulation, 2, 245-255.

Benton, J., Collins, I. R., Cooper, S. D., Grimsey, I. M., Parkinson, G. M. and Rodger, S. A. (1993) Nucleation, growth, and inhibition of barium sulphate. Faraday Discussions, 95(281), 111-115.

Dunn, K., Daniel, E., Shuler, P. J., Chen, H. J., Tang, Y. C. and Yen, T. F. (1999). Mechanisms of surface precipitation and dissolution of barite: A morphology approach. Journal of Colloid and Interface Science, 214(2), 427-437.

Graham, G. M. and L. S. Boak (2003) The influence of formation calcium and magnesium on the effectiveness of generically different barium sulphate oilfield scale inhibitors. SPE Production & Facilities, 18(1), 28-44.

He, S. L., Kan, A.T. and Thomson, M. B. (1996) Mathematical inhibitor model for barium sulfate scale control. Langmuir 12(7), 1901-1905.

Perrin, D. D. and Dempsey, B. (1974) Buffers for pH and metal ion control. London, New York, Chapman and Hall; Wiley.

Putnis, A., Putnis, C. V., and Paul, J. M. (1995) The Efficiency of a DTPA-based Solvent in the Dissolution of Barium Sulfate Scale Deposits. Proceeding of SPE International Symposium on Oilfield Chemistry, San Antonio, Texas, USA.

Sorbie, K. S., Yuan, M. D., and Jordan, M. M. (1994) Appilation of a Scale Inhibitor Squeeze Model to Improve Field Squeeze Treatment Design. European Petroleum Conference, London, England.

Yuan, M. D., Sorbie, K. S., Todd, A. C., Atkinson, L. M., Riley, H., and Gurden, S. (1993) The Modelling of Adsorption and Precipitation Scale Inhibitor

Squeeze Treatments in the North Sea Fields. SPE International Symposium on Oilfield Chemistry, New Orleans, Lousiana, USA.